AIAA JOURNAL
Vol. 42, No. 2, February 2004

Shock-Wave Mitigation Through Off-Body Pulsed Energy Deposition

Sohail H. Zaidi,* M. N. Shneider,* and R. B. Miles†
Princeton University, Princeton, New Jersey 08540

A model of dynamic shock interaction predicts that pulsed energy addition upstream of a bow shock can be used to weaken the time-averaged shock strength. To explore these shock interactions, tests have been conducted in a small-scale, blowdown facility with off-body energy addition upstream of an oblique shock wave that was generated by a wedge in a Mach 2.4 flow. The off-body energy addition was simulated by laser-induced breakdown (350 mJ/pulse with 10-ns pulse duration). The dynamics of the interactions were captured in both schlieren and shadowgraph images taken at 250,000 and 500,000 frames per second and compared with the computational model. As expected, the laser-induced thermal spot weakened the oblique shock. The images also show the dynamics of the interaction between the shock waves generated by the laser breakdown in the flow and the oblique shock, including reflections off the wedge body. The results from the near-field experiments give insight into approaches that can be used to optimize the energy addition for practical applications, including sonic boom reduction.

Introduction

THE use of continuous energy addition to the external flow around the vehicle has been considered for many years, both for drag reduction[1–6] and for sonic boom mitigation.[7,8] The drag reduction work has led to the implementation of a combustion-augmented air spike that was developed for the Trident missile back in the 1980s.[9] The concept of using off-body heating to mitigate sonic boom was proposed in the 1970s[9] but has never been implemented. In both cases, the heat was added through combustion. With the Trident, hydrogen was injected at the tip of the air spike and the flame stabilized by a disk. The presence of external burning caused substantial drag reduction. More recently, work has been done exploring the plasma arc torch concept for drag reduction[3,10] through the use of powerful off-board or on-board microwave sources. In the experiment performed by Beaulieu et al., a free, localized microwave discharge was generated upstream of a model in a Mach 1.4 flow by a focused off-board microwave beam.[11] In a work carried out by Exton et al., the plasma was generated by an on-board microwave source.[12] In that case, the microwave discharge occurred at the bow shock rather than in front of the bow shock, where energy deposition would be preferred. Tretyakov et al. were the first to use a pulsed optical discharge in a supersonic flow to affect the shock structure.[5] They conducted their work in a Mach 2 argon flow and focused a 2.5–100-kHz CO_2 laser into the flow upstream of a cylindrical model with a 60-deg angle cone. Similarly, a single laser pulse was used by Yan et al.[13] to investigate its effects on the shock-wave and flowfield structure associated with symmetric intersecting oblique shock waves. They demonstrated that as a result of energy addition, Mach stem decreased to 20% of its original height before returning to its original height.[13] Local modification of the shock structure in supersonic flows has also been demonstrated by Adelgren et al., who conducted their experiment in a Mach 3.45 facility.[14]

Pulsed energy deposition is a natural preference if high-power microwaves or laser beams are used because the power of the electromagnetic field must exceed the breakdown threshold in order to generate charge carriers for continued absorption. The powers required to achieve breakdown, even with effective focusing, usually far exceed the average power available from the device. Thus, operation in the pulse model facilitates the breakdown and leads to a further reduction in the total power required through the duty cycle of the device.

Sonic Boom and Mitigation Techniques

Shock waves generated by a supersonic object produce a sonic boom on the ground. Sonic boom formation has been the main obstacle in the development of supersonic/hypersonic vehicles. For a supersonic aircraft, the near-field shock structure is a complex array of shock waves that originates from various parts of the aircraft. In the far field these shock waves coalesce and produce an N-shape pressure signature on the ground. Although the sonic boom is a far-field phenomenon, several near-field techniques have been suggested to attenuate the shocks with the assumption that these techniques will eliminate or partially reduce the sonic boom on the ground. These techniques include the design of exceptionally long aircraft,[15] the use of underwing thermal gradients,[16] and the possibility of high-speed oscillations of flight velocity.[17] Current work focuses mainly on the development of long, thin aircraft because the other methods seem unrealistic due to practical considerations. Energy addition is an alternate approach to overcome these practical problems. It has been argued that upstream energy addition to a supersonic vehicle may weaken the shock wave and may prove to be a useful approach to suppress the sonic boom on the ground. Recent work related to the Defense Advanced Research Projects Agency (DARPA) Quiet Supersonic Platform Program, which was conducted at Princeton University, addressed these issues in greater detail. The details of this project have been presented by Miles et al.[18] The results indicated that steady-state, off-body energy addition can reduce the far-field signature primarily by suppressing the far-field coalescence of the various shock waves originating from the various parts of the vehicle.[18] The present paper contains follow-on work to that project. New theoretical and experimental results that investigate the influence of upstream pulsed energy deposition on a shock-wave structure in the near field of a model in a Mach 2.4 flow are presented. Both theoretical and experimental approaches have been adopted to investigate the complex dynamics of interaction of the entropy spot resulting from the pulsed energy deposition in the flow, with the shock wave generated from a model in the supersonic flow. The following sections describe both the experimental and theoretical approaches adopted in this study in greater detail.

Presented as Paper 2002-2703 at the AIAA 22nd Aerodynamic Measurement Technology and Ground Testing Conference, St. Louis, MO, 24–26 June 2002; received 6 September 2002; revision received 27 August 2003; accepted for publication 10 September 2003.

*Research Staff, Department of Mechanical and Aerospace Engineering.
†Head, Applied Physics, and Professor, Department of Mechanical and Aerospace Engineering.

Computational Modeling

Computational modeling was performed to investigate the dynamic effects of energy addition upstream of the shock wave produced by a model in the flow. Theoretical work was conducted at the flow conditions used for the experimental studies [$M = 2.4$, $p_0 = 1$ atm, $T_0 = 136$ K, and $\gamma = 1.4$ (ideal gas)]. In the wind-tunnel experiment a wedge of 15-mm length and a 20-deg inclusive angle was used to generate the required shock wave in the flow. However, a diamond-shaped model was used whose front half had the dimensions of the wedge employed in the experiment. The main reason for using a diamond-shaped model was to avoid the flow instabilities generated at the sharp trailing edge of the wedge and to simplify the computational calculations. A laser spark produced a cylindrical shock wave and a rarefied thermal spot that moved together downstream with the flow. The energy deposition region was assumed to have a cylindrical shape and a Gaussian distribution in the (x, z) plane with effective radius (r_{eff}) of 0.125 cm. In the experiment the laser pulse energy focused in the flow was about 350 mJ/pulse. A 40% coupling efficiency was assumed that corresponds to $Q_0 = 0.137$ J/cm, where Q_0 is the total heat dissipated by the flow per unit length in a direction normal to the flow stream.

The dynamic effects of energy addition were investigated by using a time marching two-dimensional Euler code. The set of Euler equations in Cartesian coordinates together with the ideal gas equation of state were used in the form

$$\frac{\partial}{\partial t}U + \frac{\partial}{\partial x}X + \frac{\partial}{\partial z}Z = H \tag{1}$$

$$U = \begin{Vmatrix} \rho \\ \rho u \\ \rho v \\ e \end{Vmatrix}, \qquad X = \begin{Vmatrix} \rho u \\ \rho u^2 + p \\ \rho uv \\ (e + p)u \end{Vmatrix}$$

$$Z = \begin{Vmatrix} \rho v \\ \rho uv \\ \rho v^2 + p \\ (e + p)v \end{Vmatrix}, \qquad H = \begin{Vmatrix} 0 \\ 0 \\ 0 \\ P \end{Vmatrix} \tag{2}$$

$$p = (\gamma - 1)\rho\varepsilon \tag{3}$$

$$e = \rho[\epsilon + (u^2 + v^2)/2] \tag{4}$$

where ρ and p denote the gas density and pressure, respectively; u and v are the x and z velocity components; e is the total energy of the gas per unit volume; and ϵ is the internal energy per unit mass. $P(x, z, t)$ is the power density of the source of energy released in watts per cubic meter.

Computations were performed by a widely used second-order MacCormack method (see Ref. 19) on a rectangular grid. Results were grid independent with high accuracy. (Changing mesh size by $\pm 50\%$ caused a change of about $\pm 1\%$ in the computed results.) The physical coordinates (x, z) were transformed into $(\bar{x}, \bar{z})$ according to the following transformation:

$$\bar{x} = x, \qquad \bar{z} = z/z_b(x), \qquad \bar{z} \in [0, 1] \tag{5}$$

where $z_b(x)$ is the coordinate along the upper boundary of the region of computation. On the wedge surface the velocity component normal to the wedge surface was assumed to be zero. As $\tau_{\text{pulse}} \ll L/Mc_0$, the energy deposition process can be considered as instantaneous, and therefore

$$P(x, z, t) = Q(x, z)\delta(t - t_0) \tag{6}$$

$$Q(x, z) = \left(Q_0 \big/ \pi r_{\text{eff}}^2\right) \exp\left\{-\left[(x - x_c)^2 + (z - z_c)^2\right] \big/ r_{\text{eff}}^2\right\} \tag{7}$$

where τ_{pulse} is the pulse width of the laser (10 ns), L is the length of the test section (distance between the laser focus and the oblique shock wave), c_0 is the speed of sound in the unperturbed flow, M is the Mach number, P is the released power density, Q is the spatial distribution of deposited energy, and Q_0 is the total heat per unit length dissipated by the flow.

Figure 1 presents the computational results describing the dynamics of the interaction of the energy addition with the shock wave generated by the model. The energy addition itself has generated a shock wave that grows as it propagates in the flow. The shock wave along with an thermal spot at its center can be seen propagating toward the oblique shock in frames 1–3 (Fig. 1). The complex interaction of the entropy spot with the oblique shock wave becomes more visible in frames 4–7. Frames 5 and 6 clearly show the attenuation of the shock wave as it passes through the entropy spot. The interaction of the shock wave generated by the laser spot with the oblique shock wave can also be seen clearly in frames 1–7. The laser-generated shock wave gets reflected from the wedge surface and makes the dynamics of interaction even more complex. It must be noted that the attenuation of the shock wave depends on many factors including the pulse energy and the temperature of the heating spot and the heated region in front of the shock wave. This has been thoroughly discussed in Ref. 18.

Experimental Results

An experimental program was established to validate the model predictions for the dynamic energy addition and to examine the real-time, near-field interactions of the energy addition with the shock wave produced in the flow. This was achieved by designing a small-scale Mach 2.4 blowdown facility that was developed to carry out the DARPA Quiet Supersonic Platform (QSP) program. The method of characteristics was used to design the Mach 2.4 nozzle contours. Boundary-layer calculations were taken into consideration to ensure that a uniform flow was achieved in the test section. The following nozzle design parameters were used to conduct the experimental work: Mach number 2.4, pressure ratio 14.62, test section pressure 1 atm (101.33 kPa), and throat area 1.644 in.^{2} (10.61 cm^2).

Figure 2 describes the blowdown facility layout with the test section [length 6 in., width 2.15 in. (5.461 cm), height 1.9 in. (4.826 cm)] location where the experimental work was carried out. The static pressure in the test section was near atmosphere, permitting localized energy addition by laser-induced breakdown. This relatively high pressure lowers the threshold for laser breakdown and causes the region of breakdown to remain well confined so localized energy addition can be simulated.

A wedge of 15-mm length with a 20-deg inclusive angle was introduced into the flow. The shadowgraphs and schlieren images were obtained by using a 200-mW continous wave argon-ion laser. The quality of the shadowgraphs was improved by replacing the lenses with the concave mirrors, which collimated and then refocused the beam on the screen. A 10-Hz YAG laser was employed to add the energy in the flow. The pulse energy was about 350 mJ/pulse, and a 100-mm-focal-length lens was used to obtain a breakdown in the region of interest upstream the model. A Princeton Scientific Instrument Ultra Fast Framing Camera (PSI-4) was used to capture the shock-wave interactions in the test section as the energy was added to the flow. This camera is a high-speed, solid-state imaging system that uses a PSI charge-coupled device (CCD) image sensor (80×160 pixel array). The CCD image sensor provides an on-chip storage array for 29 images (28 are usable), which can be exposed at burst rates of up to one million frames per second. The camera was operated at -20.0 to -30.0°C to reduce dark current during the readout time. Two mechanical shutters are used to provide high-speed response of the electronic shutter and the ultimate attenuation of the mechanical shutter during the readout. The video signals are digitized and sent to a data acquisition computer.

Before taking any images of the interaction between the laser-induced thermal spot and the oblique shock wave from the model, the PSI camera was tested to ensure the required performance of the system. Schlieren images of the laser spark and the associated shock wave were taken in the test section without any flow in the

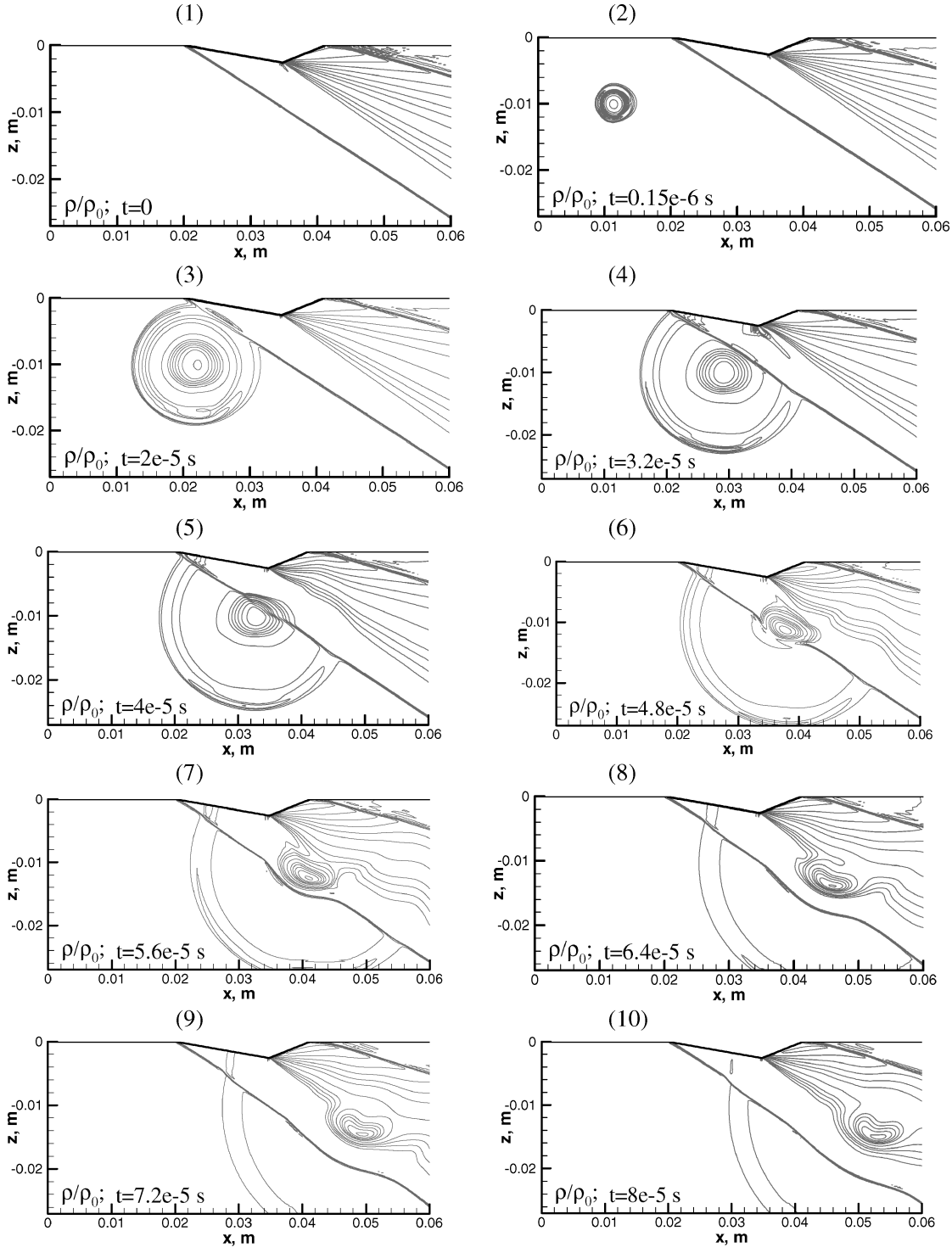

Fig. 1 Two-dimensional, time-accurate model of laser spark and the oblique shock wave interaction (density contours). Flow is from left to right.

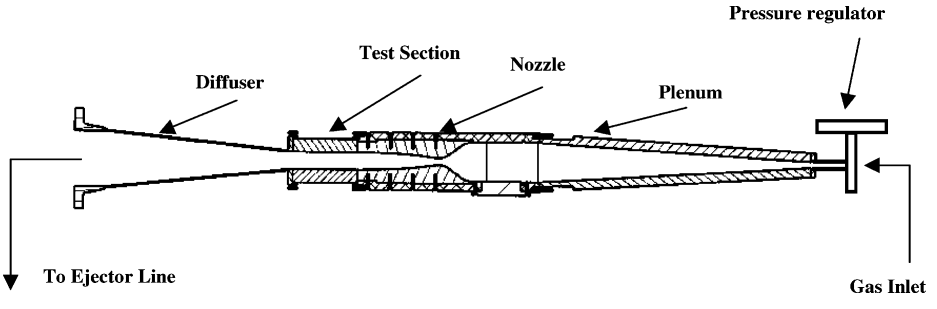

Fig. 2 Mach 2.4 blowdown facility with the test section to perform experimental work.

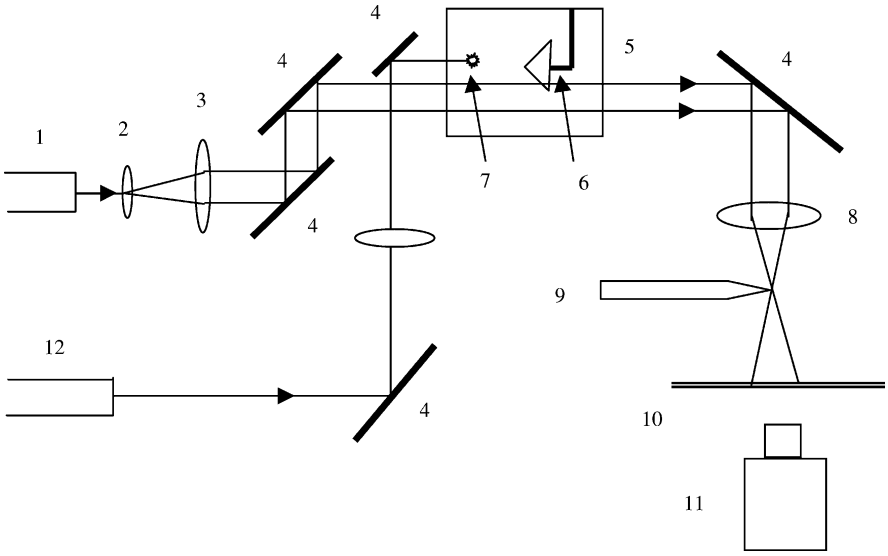

Fig. 3 Schlieren setup to image shockwaves in the test section: 1, argon ion laser; 2, microscope objective (× 10) with a pinhole of 50-μm diameter; 3, collimating lens; 4, reflecting mirrors; 5, test section; 6, model to produce shock wave; 7, laser spark; 8, focusing lens; 9, knife edge; 10, screen; 11, megahertz rate framing camera; and 12, YAG laser.

tunnel. The PCI CCD camera was operated for various integration times (from 2.0 to 16.0 μs). The camera was externally triggered from the YAG laser system that was used to a thermal spot in the tunnel. Schlieren images of the laser spark along with its associated shock wave have been presented elsewhere[20] and are not discussed in this paper.

To investigate the impact of energy addition on the shock-wave structure, the laser was focused 10 mm upstream and 10 mm below the model used for producing shock waves in the test section of the tunnel. The time-gated technique was used to capture the shock waves in the region of interest and, for this purpose, the camera trigger signal was delayed by 200 μs (relative to the laser pulse). Figure 3 describes the imaging setup along with the energy addition mechanism upstream of the model.

Figure 4 describes the experimental results as the shadowgraph images were captured with the desired flow in the tunnel. Flow is from left to right, and the laser was focused at the position 10 mm upstream and 10 mm below the model. For the results in Fig. 4, the frame integration time was 2 μs. The images in Fig. 4 clearly show the thermal spot and the associated shock waves propagating with the flow before they interact with the oblique shock wave generated by the model (frames 1–6). As the thermal spot passes through the oblique shock wave, a significant distortion and weakening of the model shock can be seen in frames 12–24. The distortion of the energy spot is also clearly visible. The full recovery of the shock wave after the thermal spot's interaction can be seen in frames 24–28.

Discussion of Results

Before going into further detail, it is important to note the remarkable agreement between the computational and experimental results presented in this work. The distortion of the oblique shock wave by the presence of the thermal spot has been seen, as was predicted by the simulation results. The experimental shadowgraph images in Fig. 4 can be compared with simulated images from dynamic models of the interaction with the same conditions. A first step in that simulation can be seen in Fig. 1, where the interaction of the localized energy deposition region with the model shock is predicted. Even though that is a two-dimensional geometry, there is a similarity in the shock bending and weakening.

As argued earlier, the interaction of the thermal spot and its associated shock wave with the oblique shock from the model is a very complicated process. In fact the shock wave associated with the thermal spot interacts with the model shock before the thermal spot itself interacts with the model shock. The shock associated with the thermal spot gets reflected from the model surface downstream to interact with the expansion fan at the right-hand edge of the model, as has been shown in Fig. 4 (frames 9–20). In the presence of interaction of two shock waves along with the interaction of the thermal spot with the model shock, it is important to predict and analyze the pressure variations in the near field, which then can be used to understand the far-field phenomenon. This was achieved by conducting a theoretical study in which localized energy addition was considered with and without the shock wave surrounding the thermal spot. Figure 5 shows the results from this calculation. The real difference between the two cases in Fig. 5 can be seen in terms of the pressure variation along the surface, 2.5 cm below the model, as shown in Fig. 6. In the case when the laser spot is focused 10 mm upstream and 10 mm below the model, the pressure variation is maximum. The rise in pressure is due to the interaction of the shock wave surrounding the thermal spot with the oblique shock wave, whereas the pressure decreases when the thermal spot interacts with the model shock. In addition, the interaction of the shock waves with the expansion fan located at the far right-hand edge of the model affects the pressure in a complicated fashion. This leads to severe fluctuations in the predicted pressure, as has been shown in Fig. 6. As the localized energy position is moved farther away from the model edge (40 mm upstream), the shock wave around the thermal spot becomes weaker and the corresponding pressure variations become smaller in amplitude, as can be seen in Fig. 6. For the isobaric case (thermal spot without any shock wave) where the pressure inside the deposition region has been assumed constant, only the interaction of the thermal spot has been analyzed. It was found that the pressure associated with the oblique shock wave reduced without any large fluctuation (Fig. 6). It is worth mentioning that for an effective sonic boom reduction, the position of the energy deposition region should be optimized such that the shock wave generated by the spot becomes weaker before it reaches the model shock. In this way the interaction of the thermal spot would have a more pronounced impact on the model shock wave. The current work suggests that the localized energy deposition at a distance of one body length upstream and one body length below the model can be considered as an optimum position for energy deposition in the flow. It is clear that far-field measurements are required to optimize the position of the energy source and to see the real impact on the sonic boom signature on the ground. Far-field measurements are beyond the scope of the current work, which was conducted in a laboratory environment to investigate the near-field effects of off-body energy addition on the shock wave that was produced by a small-scale model in a supersonic flow.

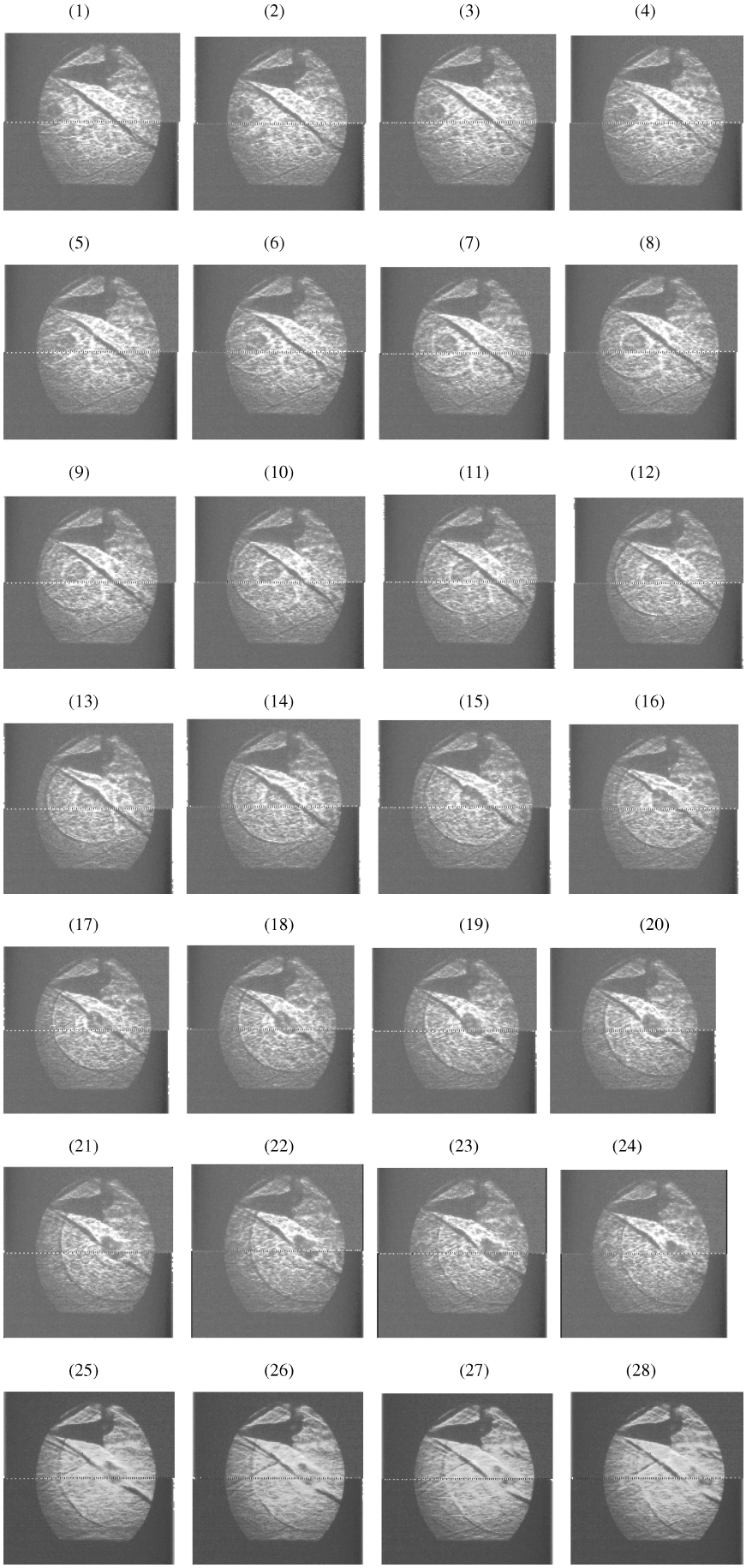

Fig. 4 Shadowgraph images of the interaction between the laser thermal spot and the oblique shock wave from a wedge in a Mach 2.4 flow. Images are 2 μs apart (frame integration time).

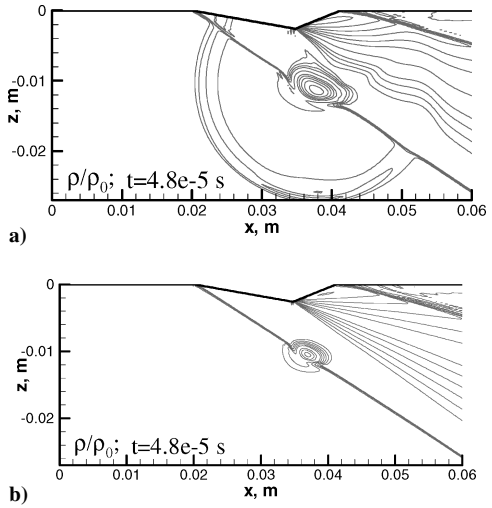

Fig. 5 Cylindrical shock wave and a) thermal spot interaction with the oblique shock at $t = 48$ μs after the laser spark and b) thermal spot–oblique shock interaction at the same time moment.

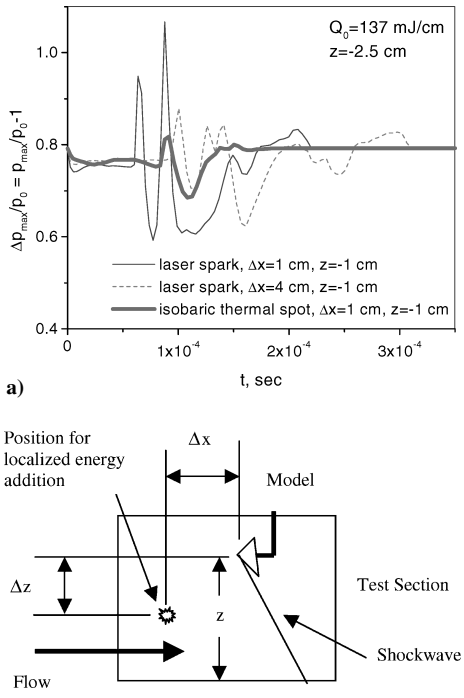

Fig. 6 Energy addition: a) computational predictions of maximum relative pressures at the bottom of the test section for various energy addition positions and b) position for localized energy addition to predict pressure variations in the model shock.

Conclusions

The interaction of the laser-induced breakdown with a model shock wave in a Mach 2.4 flow has been investigated. The computational code developed in this study predicts the weakening of the model shock as the thermal spot interacts with it. An experimental program has been launched to validate the computational results in a small-scale wind tunnel. The near-field measurements in the wind tunnel reveal the predicted interactions in a series of images that were obtained by using both the schlieren and shadowgraph techniques. A fast-framing-rate camera was used for this purpose. The experimentally observed interaction between the thermal spot and the model shock clearly indicates the weakening and bending of the model shock in the near-field region. On the basis of the experimental observations and the theoretical studies conducted in this work, it has been argued that the off-body energy addition technique can be considered as a practical way of reducing the sonic boom on the ground.

Acknowledgments

This work was initially supported by DARPA as a part of the QSP program, and continuing work is supported by the Air Force Office of Scientific Research. The authors gratefully acknowledge the important contribution of Sergey Macheret for his useful discussions on this experiment. The authors are also indebted to P. Howard for the design of the experimental rig. The work of B. Runner and L. McIntyre for machining the nozzle and the test section in the departmental workshop is gratefully acknowledged.

References

[1]Marsh, J. J., Myrabo, L. N., Messitt, D. G., and Nagamatsu, H. T., "Experimental Investigation of the Hypersonic 'Air Spike' Inlet at Mach 10," AIAA Paper 96-0721, Jan. 1996.

[2]Toro, P. G. P., Nagamatsu, H. T., Minucci, M. A. S., and Myrabo, L. N., "Experimental Pressure Investigation of a 'Directed-Energy Air Spike' Inlet at Mach 10," AIAA Paper 99-2843, July 1999.

[3]Toro, P. G. P., Nagamatsu, H. T., Myrabo, L. N., and Minucci, M. A. S., "Experimental Heat Transfer Investigation of 'Directed-Energy Air Spike' Inlet at Mach 10," AIAA Paper 99-2844, July 1999.

[4]Kuo, S. P., and Bivolaru, D., "Plasma Effect on Shock Waves in a Supersonic Flow," *Physics of Plasmas*, Vol. 8, No. 7, 2001, pp. 3258–3264.

[5]Tretyakov, P. K., Garanin, A. F., Grachev, G. N., Krainev, V. L., Ponomarenko, A. G., Tishchenko, V. N., and Yakovlev, V. I., "Supersonic Flow over Bodies Control by Using a Powerful Optical Pulsating Discharge," *Doklady Akademi Nauk*, Vol. 351, No. 3, 1996, pp. 339, 340.

[6]Yuriev, A., Pirogov, S., and Savischenko, N., "Investigation of Pulse Repetitive Energy Release Upstream Body Under Supersonic Flow," AIAA Paper 2002-2730, June 2002.

[7]Reding, J. P., and Jecmen, D. M., "Effects of External Burning on Spike-Induced Separated Flow," *Journal of Spacecraft and Rockets*, Vol. 20, No 5, 1983, pp. 452, 453.

[8]Batdorf, S. B., "Alleviation of the Sonic Boom by Thermal Means," *Journal of Aircraft*, Vol. 9, No. 2, 1972, pp. 150–156.

[9]Redding, J. P., and Jecmen, D. M., "An Advanced Aerospike to Minimize Nose Drag," *Lockheed Horizons Magazine*, Vol. 5, 1984, pp. 46–54.

[10]Bracken, R. M., Myrabo, L. N., Nagamatsu, H. T., Meloney, E. D., and Shneider, M. N., "Experimental Investigation of an Electric Arc Air-Spike with and Without Blunt Body in Hypersonic Flow," AIAA Paper 2001-0796, 2001.

[11]Beaulieu, W., Brovkin, V., Goldberg, I., Klimov, A., Kolesnichenko, Y., Krylov, A., Lashkov, V., Leonov, S., Mashek, I., Ryvkin, M., and Serov, Y., "Microwave Plasma Influence on Aerodynamic Characteristics of Body in Airflow," *Proceedings of the 2nd Weakly Ionized Gases Workshop*, edited by W.L. Bain, AIAA, Reston, VA, 1998, pp. 193–199.

[12]Exton, R. J., Balla, R. J., Shirinzaded, B., Brauckmann, G. J., Herring, G. C., Kelliher, W. C., Fugitt, J., Lazard, C. J., and Khodataev, K. V., "On-Board Projection of a Microwave Plasma Upstream of a Mach 6 Bow Shock," *Physics of Plasmas*, Vol. 8, No. 11, 2001, pp. 5013–5017.

[13]Yan, H., Adelgren, R., Elliott, G., and Knight, D., "Laser Energy Deposition in Intersecting Shocks," AIAA Paper 2002-2729, June 2002.

[14]Adelgren, R. G., Yan, H., Elliott, G. S., Knight, D., Beutner, T. J., Zheltovodov, A. A., Ivanov, M., and Khotyanovsky, D., "Localized Flow Control by Laser Energy Deposition Applied to Endy IV Shock Impingement and Intersecting Shocks," AIAA Paper 2003-0031, Jan. 2003.

[15]McLean, F. E., "Configuration Design for Specified Pressure Signature Characteristics," *Second Conference on Sonic Boom Research*, edited by I. R. Schwartz, NASA SP-180, 1968, pp. 37–40.

[16]Cheng, Sin-I, "Device for Sonic Boom Reduction and Improving Aircraft Performance," U.S. Patent 3737119, filed 15 June 1970, issued 5 June 1973.

[17]Crow, S. C., and Bergmeier, G. G. J., "Active Sonic Boom Control," *Journal of Fluid Mechanics*, Vol. 325, 1996, pp. 1–28.

[18]Miles, R. B., Martinelli, L., Macheret, S.O., Shneider, M. N., Girgis, I. H., Zaidi, S. H., and Mansfield, D. K., "Suppression of Soinc Boom by Dynamic Off-Body Energy and Shape Optimization," AIAA Paper 2002-0150, Jan. 2002.

[19]Anderson, D. A., Tannehill, J. C., and Pletcher, R. H., *Computational Fluid Mechanics and Heat Transfer*, Hemisphere, New York, 1984, pp. 102, 103.

[20]Zaidi, S. H., Shneider, M. N., Mansfield, D. K., Ionikh, Y. Z., and Miles, R. B., "Influence of Upstream Pulsed Energy Deposition on a Shock-wave Structure in Supersonic Flow," 22nd AIAA Aerodynamic Measurement Technology and Ground Testing Conf., St. Louis, MO, June 2002.

M. Sichel
Associate Editor